Adaptive Coded-Modulation in Slow Fading Channels

Young Min Kim and William C. Lindsey*

Abstract: **The adaptive coded modulation (ACM) is a promising way to provide a substantial improvement in spectral efficiency for slow fading channels. The basic idea is to adapt system functionality such as modulation, coding, information rate, and transmission power to varying channel conditions. In this work, the potential of adaptive coded modulation is investigated using cut-off rate analysis in a unified way and using computer simulation. The analysis includes various effects of fading channels such as feedback delay and channel prediction error. It was shown that the adaptive coded modulation can provide several folds of increase in spectral efficiency compared to a fixed coded-modulation system employing QPSK when channel varies slowly.**

I. INTRODUCTION

During the past decade, we have seen an explosive expansion and growth in wireless communications and a vision of communicating any-where any-time is becoming reality. Services traditionally provided by wired lines are substituted by wireless communications and vice versa. More and more portions of global communications are being serviced by wireless communications. Especially, a large portion of terminal accesses between communication networks and users is expected to be processed by radio mainly due to the freedom of being wireless. The next generation mobile radio systems, such as the Universal Mobile Telecommunications Systems (UMTS) and IMT2000 (International Mobile Telecommunications by the year 2000), are projected to support a data rate of up to a few Mbps [2]. Considering current digital mobile radio systems are being operated at a spectral efficiency less than 1 bit/sec/Hz, the spectral efficiency of future wireless systems must be increased by several times to maximize the utilization of scarce radio spectrum and offer multimedia services.

There are various methods of increasing the system capacity of cellular radio systems. Frequently adopted methods are to decrease cell size and/or to reduce the frequency reuse factor in order to reuse radio channels more in a given area. If we can double the spectral efficiency, the system capacity increase obtained from the previous methods will also be doubled. However, harsh channel conditions in cellular radio environment prevented the use of multi-level modulations such as QAM. Recently an idea of adaptive coded-modulation (ACM) was proposed by several researchers as a means of increasing the spectral efficiency of mobile radio systems [3]–[6].

The basic idea is to adapt system functionality such as modulation, coding, information rate, and transmission power to varying channel conditions. When the communication channel is time-varying, a conventional approach to communication system design is to design it based on the worst case scenario. This approach does not fully exploit the potential throughput capabilities of a fading communication channel. Another approach is to make the communication system adaptive based on the channel conditions so as to maximize the system capacity. When the channel is in a good state, we can use a coded-modulation scheme with high spectral efficiency. When the channel is poor, we can employ a robust coded-modulation scheme by trading off spectral efficiency. The channel state is observed at both the transmitter and receiver sides and the channel state information is fed back to both. As we shall see, if the adaptive procedure can be implemented successfully, we can operate the system on the average channel condition and gain significant increase in spectral efficiency. The poor spectral efficiency of current cellular radio systems stems from the fact that they were designed for the worst case channel conditions.

The idea of adaptive communication system design goes back to early 60s [1]. In [3], [4] and [7] the authors proposed an adaptive modulation scheme using Star QAM (SQAM) signal constellation. In [5] slow and fast adaptive modulations were studied in a time division duplexing (TDD) setting. TDD was adopted to provide higher correlation between the forward and reverse channels. In the slow adaptive modulation, modulation level is determined from rectangular QAM constellations during the call set-up period depending on measured carrier-to-interference (C/I) ratio and delay spread. Higher modulation level is assigned to the mobile unit nearer to the base station. Combined with dynamic channel allocation, it is reported that a significant capacity increase results [8]. In the fast adaptive modulation, modulation level is determined slot by slot based upon predicting the channel condition.

Goldsmith investigated adaptive coded-modulation schemes in [6], and [9]. In [6] variable-rate, variable-power QAM was considered to optimize both transmission rate and power in order to maximize spectral efficiency while satisfying average power and BER constraints. It was assumed that adaptation can be done perfectly symbol by symbol.

In this paper the cut-off rate of adaptive coded-modulation is analyzed for slow fading channels showing that substantial increase in spectral efficiency can be obtained. In Section II, the cut-off rate of adaptive coded-modulation is discussed under ideal assumptions. The effects of feedback delay associated with channel state estimation and channel state prediction will

Manuscript received February 4, 1999; approved for publication by Giuseppe Caire, Division I Editor, April 27, 1999.

Young Min Kim is with Communication Science Institute University of Southern California Los Angeles, CA 90089-256, USA, Tel: (213) 740-4669, Fax: (213) 740-8729, e-mail: yokim@scf.usc.edu.

William C. Lindsey is with LinCom Corporation 5110 W. Goldleaf Circle, Suite 330, Los Angeles, CA 90056, USA, Tel: (213) 293-3001, Fax: (213) 293-3063, e-mail: lindseyw@lincom.com.

This work was supported by LinCom Corporation.

* On leave of absence from the University of Southern California, Los Angeles, CA, 1998.

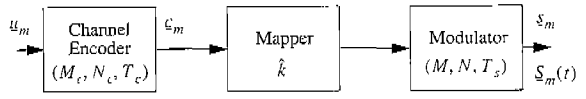

Fig. 1. A generic structure of the coded-modulator.

be studied in Section III and IV. Simulation study on the performance of adaptive-coded modulation will be also presented in VI.

II. CUT-OFF RATE OF ACM IN SLOW FADING CHANNEL

In designing coded-modulation systems, the cut-off rate plays an important role [11]. In this section, the cut-off rates of various adaptive coded-modulation systems are analyzed for slow flat Rayleigh fading channels. By slow fading it is assumed that multiplicative distortion (MD) introduced by the flat fading channel is constant over a codeword of dimension N_c. It is also assumed that the multiplicative distortion (phase and amplitude) is known at both the receiver and transmitter.

A generic coded-modulator is composed of 3 blocks: a channel encoder, a mapper and a modulator, as shown in Fig. 1 [10]. A message m generates K_c information symbols $\underline{u}_m = (u_{m1}, u_{m2}, \ldots, u_{mK_c})$ where each u_{mi} is one of Q-ary alphabet. So, the number of messages that can be transmitted is $M_c = Q^{K_c}$. Each message is then encoded into a codeword $\underline{c}_m = (c_{m1}, c_{m2}, \ldots, c_{mN_c})$, where N_c is the dimensionality of the codeword. Each code symbol c_{mi} is also from Q-ary alphabet. When $N_c > K_c$, redundancy is introduced by the channel encoder, and the code rate r_c is given by

$$r_c = \frac{\log_2 M_c}{N_c} = \frac{K_c \log_2 Q}{N_c} \quad \text{[bits/dimension]}. \tag{1}$$

If we let T be a time span of information block of length K_c, $T = T_b K_c \log_2 Q$ where T_b is the time spent per information bit, and the codeword dimension N_c can be given by

$$N_c = (T_b/T_c) K_c \log_2 Q, \tag{2}$$

where T_c is the time used for each codeword dimension.

The modulator has a set of waveforms $\{s_l(t) : l = 0, 1, \ldots, M-1\}$. Each waveform $s_l(t)$ has a duration of T_s and spans an N-dimensional space. In vector form, $\underline{s}_l = (s_{l1}, s_{l2}, \ldots, s_{lN})$. The mapper uses the modulator $\hat{k}$ times to generate the waveform $S_m(t)$ for the message m, and $T = \hat{k} T_s$. In vector form, $\underline{S}_m = (\underline{S}_{m1}, \underline{S}_{m2}, \ldots, \underline{S}_{m\hat{k}})$ where each $\underline{S}_{mi}$ is one of $\{\underline{s}_l : l = 0, 1, \ldots, M-1\}$. In the following, we assume that mapping between codeword and modulated waveform is isometric and that $Q = M$. So, $\hat{k} = N_c$ and $T_s = T_c$.

For the modulation signal set, we consider a signal set containing L signal points. The signal set can be formed from SQAM, QAM or MPSK signal constellation. It is assumed that $|\underline{s}_l|^2 \le E_c$ where E_c is the peak energy per codeword dimension.

When a message m is transmitted, the received signal $\underline{r}$ is given by

$$\underline{r} = \hat{\alpha} \underline{S}_m + \underline{n}, \tag{3}$$

where $\hat{\alpha}$ is the amplitude of the MD induced by the slow flat fading channel and $\underline{n}$ is the AWGN with two-sided spectral density $N_0/2$. It is assumed that the MD is constant over a codeword of duration T and that the channel distortion is corrected without error at the receiver. The MD is assumed to have a Rayleigh pdf: $f(\hat{\alpha}) = (\hat{\alpha}/\sigma^2) \exp(-\hat{\alpha}^2/2\sigma^2)$ where $\sigma^2 = E\{\hat{\alpha}^2\}/2$ and $\hat{\alpha} \ge 0$.

It is assumed that $\hat{\alpha}$ is also known to the transmitter, and that knowledge is utilized at the transmitter for adaptive coded-modulation. That is, the transmitter is assumed to have the ability to select the best coded-modulation scheme depending on the channel state. Suppose that the transmitter uses a coded-modulation scheme C_l when $\hat{x}_{l-1} \le \hat{\alpha} < \hat{x}_l$. Then, for the selected coded-modulation scheme C_l, the pairwise probability of error (PPE) $P_2(m, k|C_l)$, the probability that the receiver will decode the received signal to the message k when the message m is transmitted, is

$$P_2(m, k|C_l) = \frac{1}{\Pr(A_l)} \int_{\hat{x}_{l-1}}^{\hat{x}_l} P_2(m, k|\hat{\alpha}, C_l) f(\hat{\alpha}) d\hat{\alpha}, \tag{4}$$

where A_l is the event that $\{\hat{x}_{l-1} \le \hat{\alpha} < \hat{x}_l\}$ and $P_2(m, k|\hat{\alpha}, C_l)$ is the PPE given $\hat{\alpha}$. The conditional PPE $P_2(m, k|\hat{\alpha}, C_l)$ can be upper-bounded by

$$P_2(m, k|\hat{\alpha}, C_l) \le \prod_{n=1}^{N_c} \exp\left(-\hat{\alpha}^2 \frac{|S_{mn} - S_{kn}|^2}{4N_0}\right), \tag{5}$$

assuming that $\hat{\alpha}$ is known to the receiver. Following the random coding argument in [10], the ensemble error probability $\overline{P(E|C_l)}$ given C_l can be upper-bounded by

$$\overline{P(E|C_l)} < \frac{M_c}{\Pr(A_l)} \int_{\hat{x}_{l-1}}^{\hat{x}_l} \left[\frac{1}{L^2} \times \sum_{i=1}^{L} \sum_{j=1}^{L} \exp\left(-\hat{\alpha}^2 E_c \frac{|\underline{z}_i - \underline{z}_j|^2}{4N_0}\right)\right]^{N_c} f(\hat{\alpha}) d\hat{\alpha}, \tag{6}$$

where $\underline{z}_i = \underline{s}_i/\sqrt{E_c}$ and each $\underline{s}_i$ is assumed to be equally-likely. Let $\alpha = \hat{\alpha}/\sqrt{2\sigma^2}$, $x_l = \hat{x}_l/\sqrt{2\sigma^2}$, and denote $E_{N_c} = 2\sigma^2 E_c$. Then,

$$\overline{P(E|C_l)} < \frac{M_c}{\Pr(A_l)} \int_{x_{l-1}}^{x_l} \left[\frac{1}{L^2} \times \sum_{i=1}^{L} \sum_{j=1}^{L} \exp\left(-\alpha^2 E_{N_c} \frac{|\underline{z}_i - \underline{z}_j|^2}{4N_0}\right)\right]^{N_c} f(\alpha) d\alpha, \tag{7}$$

while $f(\alpha) = 2\alpha \exp(-\alpha^2)$.

Denoting

$$G(\alpha) = \frac{1}{L^2} \sum_{i=1}^{L} \sum_{j=1}^{L} \exp\left(-\alpha^2 E_{N_c} \frac{|\underline{z}_i - \underline{z}_j|^2}{4N_0}\right) \tag{8}$$

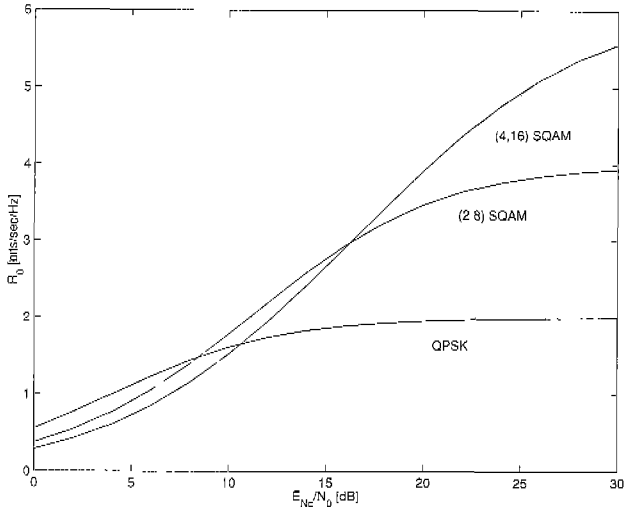

Fig. 2. Average cut-off rate of ACM with SQAMs in the slow fading channel.

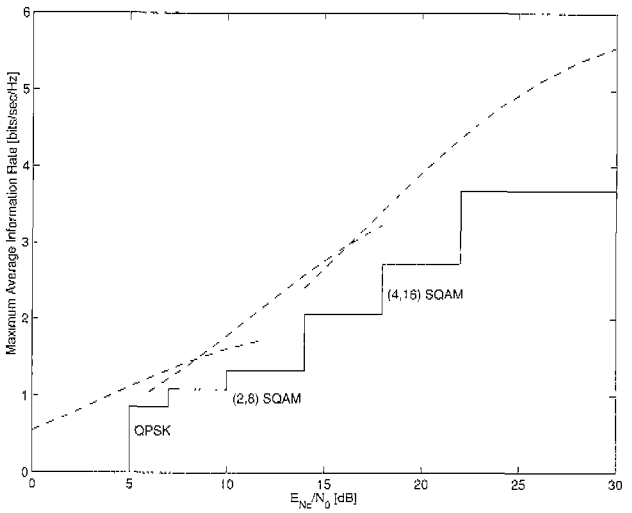

Fig. 3. The maximum average information rate of ACM with SQAMs in the slow fading channel with $J = 3$ channel codes for each modulation.

and supposing that $\Delta\alpha = x_l - x_{l-1}$ is infinitesimal, then the conditional cut-off rate $R_{0,l}$ can be approximated as

$$R_{0,l} \approx -\log_2 G(\alpha_l) \tag{9}$$

and the average cut-off rate R_0 is given by

$$R_0 = \sum_{l=1}^{\infty} R_{0,l} \Pr(A_l). \tag{10}$$

Fig. 2 shows the average cut-off rate for different modulations in the slow fading channel. In the figures, (A, P) SQAM represents a SQAM with A amplitude levels and P phase values. We can see that one modulation scheme provides larger average cut-off rate than other modulation schemes depending on the level of E_{N_c}/N_0. Noting that the signal-to-noise (or interference) ratio (SNR or SIR) is a time- and/or location-dependent quantity in time-varying channels, we can adapt modulation to SNR to maximize information transfer rate.

The average cut-off rate predicted above will be achieved if we can seamlessly adapt coded-modulation to continuously varying fading level. This will impose too much complexity in the transceiver. We propose a more practical adaptive coded-modulation as follows. Given a modulation optimized to a given SNR level, J coding schemes are combined with that modulation and the j^{th} coding scheme is operated when $x_{j-1} \leq \alpha < x_j$. Being conservative somewhat, let's assume that the code rate of the j^{th} coding scheme is $R_{0,j-1}$ and the maximum average information rate Ω achievable will be

$$\Omega = \sum_{j=1}^{J} R_{0,j-1} \Pr(x_{j-1} \leq \alpha < x_j) \quad \text{[bits/sec/Hz]}. \tag{11}$$

Fig. 3 illustrates the maximum average information rate using $J = 3$ coding schemes with the modulations discussed in Fig. 2. For each adaptive coded-modulation scheme, the operational boundaries x_j were selected so as to maximize Ω. The staircase curves are obtained because discrete SNR levels are used in optimizing the adaptive coded-modulation.

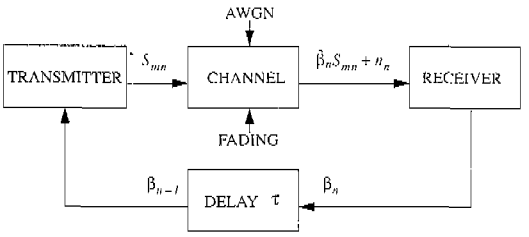

Fig. 4. A system model for an adaptive modulation scheme with feedback delay.

A conventional non-adaptive coded-modulation should fix its code rate to a $R_{0,l}$ value at a target SNR level, and its achievable information rate will be fixed at $R_{0,l} \Pr(\alpha \geq x_l)$ when E_{N_c}/N_0 is greater than the target SNR value. As a result, a substantial portion of channel capacity can not be utilized.

III. EFFECTS OF FEEDBACK DELAY

In the previous section, the feedback delay associated with channel state information was assumed to be zero. In this section, the effect of feedback delay is evaluated using different models for the correlation in fading channels, and the required channel conditions for satisfactory operation of the ACM system in correlated fading channels are discussed.

Given the previous channel state information, a coded modulation scheme should be based on this information. A simplified system model is shown in Fig. 4. The multiplicative distortion $\hat{\beta}_n$ at time n is given by $\hat{\beta}_n = \hat{\alpha}_n \exp(j\theta_n)$, and its normalized version is defined as $\beta_n = \hat{\beta}_n / \sqrt{(2\sigma^2)}$ where $E\{\hat{\beta}_n^2\} = E\{\hat{\alpha}_n^2\} = 2\sigma^2$. The channel state is assumed to be fed back to the transmitter lagged by l time units.

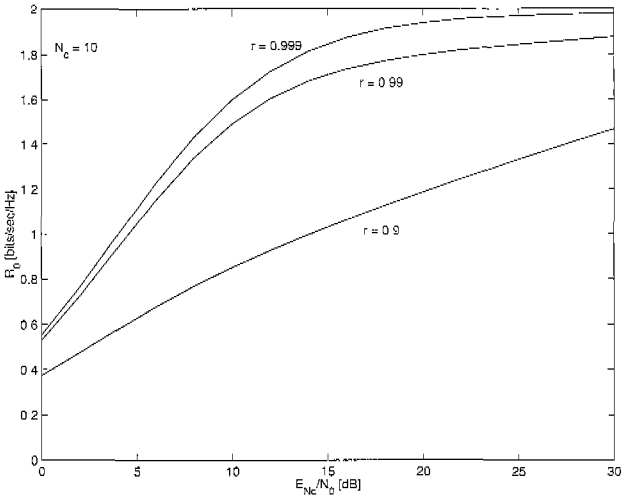

Fig. 5. Average cut-off rates of 4-ary coded QPSK ACM for different values of ρ when $N_c = 10$.

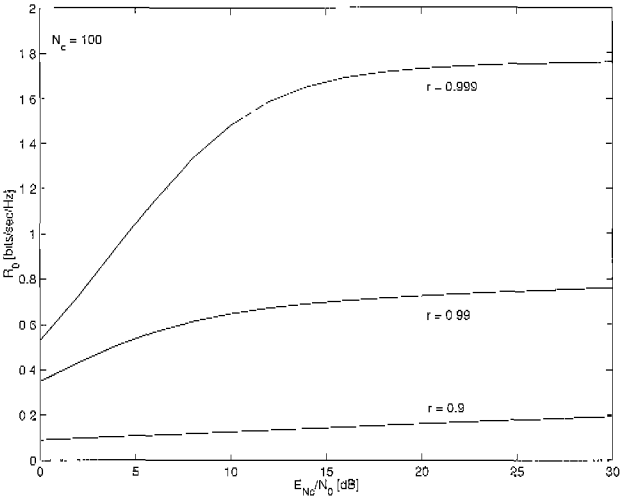

Fig. 6. Average cut-off rates of 4-ary coded QPSK ACM for different values of ρ when $N_c = 100$.

A. *Quasi-Static Fading Channel*

By quasi-static fading channel, we mean that the multiplicative distortion is constant over a codeword of length N_c while changing between codewords with a given correlation. That is, $\beta_n = \beta_0$ for $n = 0, 1, \ldots, N_c - 1$ and it is assumed that $E\{\beta_n \beta_{n-l}\} = \rho$.

Given a delayed channel state information (α_{-l}), it can be easily shown that the probability density function of current channel state (α_0) can be modeled by

$$f(\alpha_0|\alpha_{-l}) = \frac{2\alpha_0}{1-\rho^2} \exp\left\{-\frac{\alpha_{-l}^2\rho^2 + \alpha_0^2}{(1-\rho^2)}\right\} I_0\left(\frac{2\alpha_{-l}\alpha_0\rho}{1-\rho^2}\right), \tag{12}$$

assuming Rayleigh fading. In (12) the correlation coefficient ρ is assumed to be $J_0(2\pi f_d \tau)$ where f_d is the Doppler frequency, $\tau = lT_s$, and $J_0(t)$ is the 0th order Bessel function of the 1st kind.

Noting that the current fading amplitude α_0 conditioned on the feedback α_{-l} has the pdf given in (12), the pairwise probability error $P_2(m, k|\alpha_{-l})$ conditioned on α_{-l} can be upper-bounded by

$$P_2(m, k|\alpha_{-l}) < \int_0^\infty \prod_{n=0}^{N_c-1} \exp\left(-\alpha_0^2 \frac{E_{N_c}}{4N_0}|\underline{z}_{mn} - \underline{z}_{kn}|^2\right) \times f(\alpha_0|\alpha_{-l}) d\alpha_0. \tag{13}$$

Let's denote the right hand side of (13) as $P_2^u(m, k|\alpha_{-l})$. Then,

$$P_2^u(m, k|\alpha_{-l}) = \frac{\exp\left[-\frac{\alpha_{-l}^2\rho^2 \sum_{n=0}^{N_c} K_n}{(1-\rho^2)\sum_{n=0}^{N_c} K_n + 1}\right]}{(1-\rho^2)\sum_{n=0}^{N_c} K_n + 1}, \tag{14}$$

where

$$K_n = \frac{E_{N_c}}{4N_0}|\underline{z}_{mn} - \underline{z}_{kn}|^2. \tag{15}$$

The ensemble average error probability $\overline{P(E|\alpha_{-l})}$, conditioned on the previous channel condition, is obtained by averaging $P_2(m, k|\alpha_{-l})$ over all possible pairs of code or channel symbol sequences. Let's assume that $|\underline{z}_{mn} - \underline{z}_{kn}|^2 \in \{d_1^2, d_2^2, \ldots, d_q^2\}$, *i.e.*, there are q different squared Euclidean distances for given modulation symbol set. If $p_i = \Pr(|\underline{z}_{mn} - \underline{z}_{kn}|^2 = d_i^2)$ and n_i is the number of positions with d_i^2, $\overline{P(E|\alpha_{-l})}$ can be upper-bounded by

$$\overline{P(E|\alpha_{-l})} < \sum_{\substack{n_1, n_2, \ldots, n_q \\ n_1+n_2+\cdots+n_q=N_c}} \binom{N_c}{n_1 n_2 \ldots n_q} p_1^{n_1} p_2^{n_2} \ldots p_q^{n_q} \times P_2^u(m, k|\alpha_{-l}), \tag{16}$$

where $\binom{N_c}{n_1 n_2 \ldots n_q}$ is the multi-nomial coefficients. Denoting the right hand side of the (16) as $\overline{P^u(E|\alpha_{-l})}$, the cut-off rate $R_{0,l}$, conditioned on α_{-l}, is given by

$$R_{0,l} = -\frac{1}{N_c} \log_2 \overline{P^u(E|\alpha_{-l})}, \tag{17}$$

similarly as in the previous section. The average cut-off rate R_0 is then obtained by averaging over α_{-l}. The major difference from the ideal case in Section II is that the cut-off rate now depends on the codeword dimension N_c.

Fig. 5 and 6 show the average cut-off rate R_0 for different correlation values when $N_c = 10$ and $N_c = 100$. In both cases, the average cut-off rate is drastically degraded when the correlation ρ (in the figures labeled as r) is not high enough. As N_c increases to 100 from 10, a higher value of ρ is required to achieve a comparable level of R_0.

If we look at the expression in (14) more closely, we can see that the error probability is inverse-linearly proportional to the signal-to-noise ratio E_{N_c}/N_0 unless $\rho = 1$. As ρ approaches to 1, the exponent in (14) becomes dominated by the numerator term and the error probability becomes inverse-exponentially proportional to E_{N_c}/N_0. On the other hand, as N_c increases, the term $\sum_{n=0}^{N_c} K_n$ in (14) also increases, and a higher value of

ρ is required to make the term $(1-\rho^2)\sum_{n=0}^{N_c} K_n$ negligible, which will give an exponential behavior of the error probability. From this results, we can see that the codeword dimension N_c is a system design parameter which should be selected carefully depending on the channel state correlation between consecutive codeword transmissions.

B. Correlated Fading Channel

Now we drop the assumption that the fading level is constant over a codeword. The vector $\underline{\beta} = (\beta_0, \beta_1, \ldots, \beta_{N_c-1})^T$ is a column vector that represents the multiplicative distortion process. The covariance matrix $V = E\{\underline{\beta}\underline{\beta}^H\}$ where H denotes complex conjugate transpose operation, and we assume that its ith row jth column element $V_{ij} = J_0(2\pi f_d|i-j|T_s)$. The correlation $\underline{p}$ between $\underline{\beta}$ and β_{-l} is given by $\underline{p} = E\{\underline{\beta}\beta_{-l}^*\}$ and its ith element $p_i = J_0(2\pi f_d|i+l|T_s)$.

Similarly as in Section III-A the conditional pairwise probability of error $P_2(m,k|\beta_{-l})$ can be upper-bounded by

$$P_2(m,k|\beta_{-l}) < \int_{C^{N_c}} \prod_{n=0}^{N_c-1} \exp(-|\beta_n|^2 K_n) f(\underline{\beta}|\beta_{-l}) d\underline{\beta}, \tag{18}$$

where $d\underline{\beta}$ denotes $d\beta_1 d\beta_2 \ldots d\beta_{N_c}$. It is assumed that $\underline{\beta}$ is a circularly-symmetric complex Gaussian random vector. Hence, the conditional probability density function is given by

$$f(\underline{\beta}|\beta_{-l}) = \frac{\exp\left[-(\underline{\beta}-\mu)^T W^{-1}(\underline{\beta}-\mu)\right]}{\pi^{N_c}\det(W)}, \tag{19}$$

where covariance matrix $W = (V - \underline{p}\underline{p}^T)$ and mean vector $\mu = \beta_{-l}\underline{p}$. Noting that the integration in (18) gives the characteristic function of a quadratic form of circularly-symmetric complex Gaussian vector [14], we have

$$P_2(m,k|\beta_{-l}) < \frac{\det(Z)}{\det(W)} \exp\left[-\frac{1}{2}|\beta_{-l}|^2 \underline{p}^T \left\{W^{-1} - (2WKW+W)^{-1}\right\}\underline{p}\right], \tag{20}$$

where $Z = (K + \frac{1}{2}W^{-1})^{-1}$ and K is a diagonal matrix whose nth diagonal element is K_n.

An upper-bound of the ensemble average error probability $\overline{P(E|\beta_{-l})}$, conditioned on β_{-l}, is obtained by averaging $P_2(m,k|\beta_{-l})$ over all possible pairs of channel symbol sequences. Given $\overline{P(E|\beta_{-l})}$, the conditional cut-off rate $R_{0,l}$ can be computed using (17), and the maximum average information rate using (11).

For larger values of N_c, it takes a long computing time to calculate $R_{0,l}$ even for a simple modulation such as QPSK. We circumvent this computing problem using a slightly different channel model presented in the next subsection.

C. Markovian Fading Channel

Let's assume that the channel state at time k depends only on the channel state at time $k-1$ when conditioned on the previous channel states, that is,

$$f(\beta_k|\beta_{k-1}, \beta_{k-2}, \ldots) = f(\beta_k|\beta_{k-1}).$$

Letting $\rho_0 = E\{\beta_0\beta_{-l}^*\}$ and $\rho_1 = E\{\beta_k\beta_{k-1}^*\}$, the conditional pdf $f(\beta_0|\beta_{-l})$ is characterized with mean $\rho_0\beta_{-l}$ and variance $(1-\rho_0^2)$ and the conditional pdf $f(\beta_k|\beta_{k-1})$ has mean $\rho_1\beta_{k-1}$ and variance $(1-\rho_1^2)$.

Then, the upper-bound of $P_2(m,k|\beta_{-l})$ in (18) can be evaluated recursively using the following expression

$$P_2(m,k|\beta_{-l}) = \frac{1}{\sqrt{1+\hat{K}_0(1-\rho_0^2)}} \times \prod_{n=1}^{N_c-1} \frac{1}{\sqrt{1+\hat{K}_n(1-\rho_1^2)}} \exp\left[-\frac{\hat{K}_0\rho_0^2\beta_{c,-l}^2}{1+\hat{K}_0(1-\rho_0^2)}\right], \tag{21}$$

where

$$\hat{K}_{N_c-k} = \frac{\hat{K}_{N_c-k+1}\rho_1^2}{1+\hat{K}_{N_c-k+1}(1-\rho_1^2)} + K_{N_c-k}. \tag{22}$$

for $k = 2, 3, \ldots, N_c$ and $\hat{K}_{N_c-1} = K_{N_c-1}$.

With these results, we can compute the conditional cut-off rate $R_{0,l}$, the average cut-off rate R_0, and the maximum average information rate as before.

Fig. 7 and 8 show the average cut-off rate of 4-ary coded QPSK ACM for different normalized Doppler (ND) when $N_c = 64$ and 256. The normalized Doppler is defined to be f_dT_s. Feedback delay of $5N_cT_s$ sec is assumed. We observe the same behavior as in Section III-A as N_c increases. Higher correlation values are required for the ACM to work properly as the codeword length becomes longer. In the case of no feedback delay, ρ_0 was set to be 1 in calculating the average cut-off rate. The result demonstrates that most of the degradation comes from feeding delayed channel state information. In the next section, this issue of feeding back timely channel condition is investigated by incorporating channel state prediction into system.

Fig. 9 shows the average cut-off rate of 4-ary coded QPSK ACM for different normalized Doppler (ND) when $N_c = 256$ and feedback is error-free. As the normalized Doppler increase, the average cut-off rate is degraded significantly even with the assumption of error-free feedback of channel state.

IV. ACM WITH CHANNEL PREDICTION

To provide high correlation between the fed-back and current channel states, we need to feed back the predicted channel state instead of the one that is out-of-date. In this section, the average cut-off rate of ACM is analyzed with the Wiener filter used for the channel state predictor assuming that the correlation function of the channel process is known to the receiver.

Observed signal vector at the nth block $\underline{\gamma}_n = (\gamma_{n-1}, \gamma_{n-2}, \cdots, \gamma_{n-O})^T$ is the input to the channel state predictor as shown in Fig. 10 when the order of the Wiener filter is O. Suppose that there are N_{pp} pilots available for each block of codeword length N_c, and the observed signal γ_{n-k} is given by

$$\gamma_{n-k} = \frac{1}{N_{pp}}\sum_i \beta_i + \frac{1}{s_p}n_i, \tag{23}$$

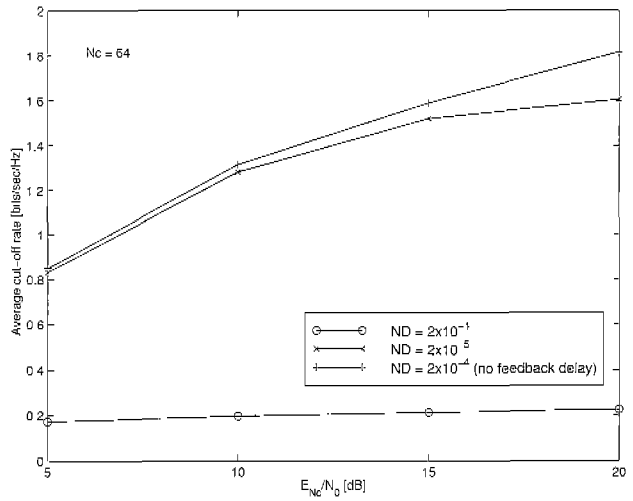

Fig. 7. Average cut-off rate of 4-ary coded QPSK ACM for different normalized Doppler (ND) when $N_c = 64$. Feedback delay is $5N_cTs$ sec.

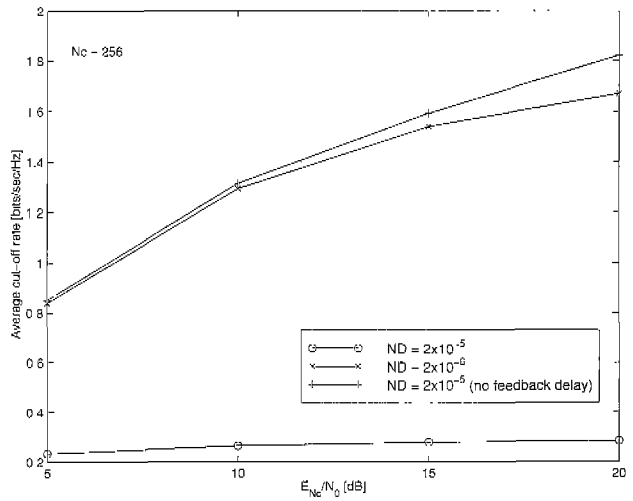

Fig. 8. Average cut-off rate of 4-ary coded QPSK ACM for different normalized Doppler (ND) when $N_c = 256$. Feedback delay is $5N_cTs$ sec.

where s_p is the pilot signal and the summation is over the N_{pp} received signals associated with the pilots in the previous $n-k$th block.

Let $R_\gamma = E\{\underline{\gamma}\underline{\gamma}^H\}$ and $\underline{p}_\gamma = E\{\underline{\gamma}\beta_0^*\}$. Assuming these correlation matrix and vector are known to the receiver, the Wiener filter coefficient vector $\underline{w}$ is given by [13]

$$\underline{w} = R_\gamma^{-1}\underline{p}_\gamma \tag{24}$$

and the channel state prediction estimate $\hat{\beta}_0$ can be obtained by

$$\hat{\beta}_0 = \underline{w}^H\underline{\gamma}. \tag{25}$$

To evaluate the effect of channel state prediction error on the average cut-off rate of ACM, we need to know the conditional probability density function $f(\beta_0|\hat{\beta}_0)$. Let's denote the complex numbers β_0 and $\hat{\beta}_0$ in vector form: $\beta_0 = (\beta_{c0}, \beta_{s0})^T$ and $\hat{\beta}_0 = (\hat{\beta}_{c0}, \hat{\beta}_{s0})^T$ where the subscripts c and s represent the real and imaginary parts, respectively. Then, since β_0 and $\hat{\beta}_0$ are jointly Gaussian, the conditional pdf $f(\beta_0|\hat{\beta}_0)$ can be given by

$$f(\beta_0|\hat{\beta}_0) = N\left(K_{\beta_0\hat{\beta}_0}K_{\hat{\beta}_0}^{-1}\hat{\beta}_0, K_{\beta_0} - K_{\beta_0\hat{\beta}_0}K_{\hat{\beta}_0}^{-1}K_{\hat{\beta}_0\beta_0}\right), \tag{26}$$

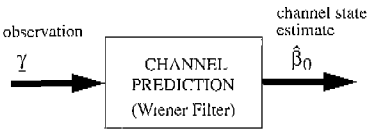

Fig. 10. Channel prediction based on the Wiener filter.

where K_{xy} is the cross-covariance matrix of x and y, K_x is the covariance matrix of x, and $N(\underline{m}, K)$ denotes the vector normal density with mean vector $\underline{m}$ and covariance matrix K. Noting that $\underline{\beta}_{cp}$ and $\underline{\beta}_{sp}$ are independent of each other, the covariance and cross-covariance matrices are given by

$$K_{\beta_0} = \begin{bmatrix} 1/2 & 0 \\ 0 & 1/2 \end{bmatrix}, \quad K_{\beta_0\hat{\beta}_0} = \frac{1}{4}\underline{p}_\gamma^T R_\gamma^{-1}\underline{p}_\gamma \begin{bmatrix} 1 & -1 \\ 1 & 1 \end{bmatrix} = K_{\hat{\beta}_0\beta_0}^T,$$
$$\text{and} \quad K_{\hat{\beta}_0} = \frac{1}{4}\underline{p}_\gamma^T R_\gamma^{-1}\underline{p}_\gamma \begin{bmatrix} 1 & 0 \\ 0 & 1 \end{bmatrix}. \tag{27}$$

Let the conditional covariance matrix $K_{\beta_0|\hat{\beta}_0} = K_{\beta_0} - K_{\beta_0\hat{\beta}_0}K_{\hat{\beta}_0}^{-1}K_{\hat{\beta}_0\beta_0}$ and the conditional mean vector $\underline{m}_{\beta_0|\hat{\beta}_0} = (m_c, m_s)^T = K_{\beta_0\hat{\beta}_0}K_{\hat{\beta}_0}^{-1}\hat{\beta}_0$. Using the results in (27),

$$K_{\beta_0|\hat{\beta}_0} = \frac{1}{2}\left(1 - \underline{p}_\gamma^T R_\gamma^{-1}\underline{p}_\gamma\right)\begin{bmatrix} 1 & 0 \\ 0 & 1 \end{bmatrix}$$
$$\text{and} \quad \underline{m}_{\beta_0|\hat{\beta}_0} = \begin{bmatrix} \hat{\beta}_{c0} - \hat{\beta}_{s0} \\ \hat{\beta}_{c0} + \hat{\beta}_{s0} \end{bmatrix}. \tag{28}$$

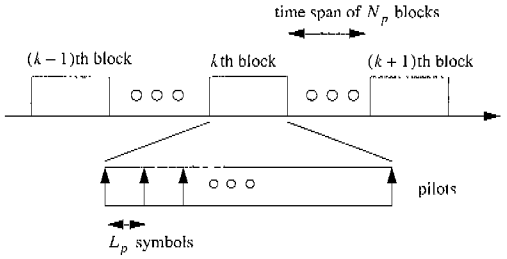

Fig. 11. A pilot symbol configuration: equally-spaced pilots.

So, given $\hat{\beta}_0$, β_{c0} and β_{s0} are independent, and the conditional pdf $f(\beta_0|\hat{\beta}_0)$ can be decomposed into

$$f(\beta_0|\hat{\beta}_0) = N\left(m_c, \frac{1}{2}(1-\hat{\rho}^2)\right) N\left(m_s, \frac{1}{2}(1-\hat{\rho}^2)\right), \tag{29}$$

where

$$\hat{\rho}^2 = \underline{p}_\gamma^T R_\gamma^{-1} \underline{p}_\gamma. \tag{30}$$

If we use this conditional pdf at the final step of the recursive procedure of computing the conditional cut-off rate $R_{0,l}$ as in Section III-C, the conditional ensemble error probability $\overline{P(E|\hat{\beta}_0)}$ can be upper-bounded by

$$\overline{P(E|\hat{\beta}_0)} < \frac{1}{1+\hat{K}_0(1-\hat{\rho}_0^2)} \times \prod_{n=N_c-1}^{1} \frac{1}{1+\hat{K}_n(1-\rho_1^2)} \exp\left[-\frac{(m_c^2+m_s^2)\hat{K}_0}{1+\hat{K}_0(1-\hat{\rho}_0^2)}\right]. \tag{31}$$

Note that the right hand side of the inequality given above depends only on the magnitude of $\hat{\beta}_0$ instead of $\hat{\beta}_0$ because $(m_c^2+m_s^2) = 2|\hat{\beta}_0|^2$.

One more difference from the result in the previous section is that the fed-back channel state information $\hat{\beta}_0$ is a complex Gaussian random variable with variance $\hat{\rho}^2$ while β_{-l} with variance 1. So, the pdf of the amplitude of $\hat{\beta}_0$ is given by

$$f(|\hat{\beta}_0|) = \frac{2|\hat{\beta}_0|}{\hat{\rho}^2} \exp\left(-\frac{|\hat{\beta}_0|^2}{\hat{\rho}^2}\right). \tag{32}$$

Using this pdf, the maximum average information rate of ACM with channel prediction can be given by

$$\Omega = \sum_l R_{0,l} \Pr\{|\hat{\beta}_0| \in B_l\}, \tag{33}$$

where B_l is the range of $|\hat{\beta}_0|$ over which the lth coded-modulation operates.

For numerical evaluation of the maximum average information rate in (33), we consider a pilot symbol arrangement illustrated in Fig. 11. For each block, N_{pp} pilots are equally spaced, and each block is separated by time a span of N_p blocks. The pilots in each block are L_p symbols apart. Fig. 12 shows the maximum average information rate of a 4-ary coded QPSK ACM

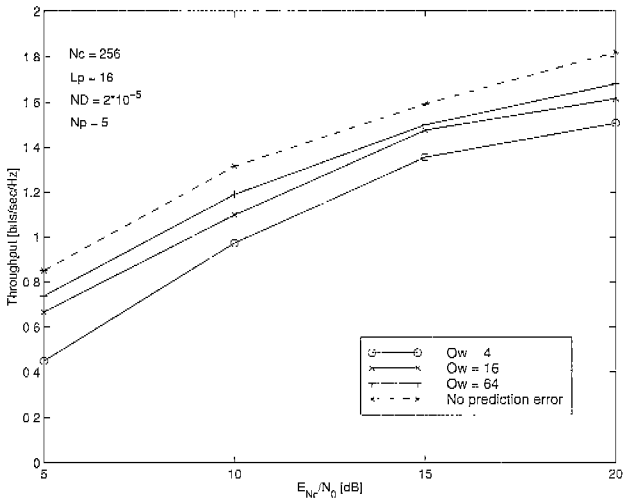

Fig. 12. A 4-ary coded QPSK ACM with channel prediction.

when $N_c = 256$, $L_p = 16$, $N_p = 5$, and the normalized Doppler frequency is 2×10^{-5}. Also shown is the case with no feedback delay and no channel prediction error. As we increase the order of the Wiener filter to 64, most of the channel capacity attainable in the ideal case is achieved under the conditions considered.

Based on the result obtained so far, we can identify the channel conditions and system parameters for which the adaptive coded-modulation will improve the information transfer rate well over the one possible with conventional fixed coded-modulation schemes.

V. ACM IN DIVERSITY CHANNELS

It is well known that diversity techniques are efficient in mitigating fading effects [14]. Under fading, radio communication systems suffer from a severe performance degradation because the received signal power level could drop by more than 20 dB and the probability of that occurrence is not negligible. However, when more than one independent copies of transmitted signals are available at the receiver, we can improve the signal-to-noise ratio and reduce the probability of deep fades by using diversity combining techniques.

There are various diversity techniques such as frequency, time, path, polarization and space diversities depending on the way by which the receiver obtains independent multiple copies of the transmitted signal. Among these possible schemes, we consider only space diversity in this work. Space diversity has advantages over other diversity techniques. Unlike frequency or time diversity, it can increase diversity order as much as we want without requiring additional channel resource. Polarization or path diversity has a limitation in diversity order that can be achieved.

On the other hand, in the applications where radio spectrum is reused over different geographical areas and cochannel interference (CCI) is unavoidable as in cellular radio systems, diversity technique is also very effective in suppressing cochannel interference which is often dominant limiting factor in system performance. So, the effect of cochannel interference is also included in the performance analysis of ACM in diversity channels.

A. *Average Cut-Off Rate of ACM with Maximal Ratio Combining*

Consider that there are D antennas at the receiver separated with enough spacing to provide independence between signals at different antenna branch, so diversity order is D. In complex baseband equivalent model, the received signal $r_l(n)$ at the lth antenna branch at time n is given by

$$r_l(n) = s_{0l}(n) + \sum_{k=1}^{N_i} s_{kl} + v_l(n), \tag{34}$$

where $s_{kl}(n)$ is the kth user's signal and $v_l(n)$ is complex AWGN at the lth branch. Suppose that s_{0l} is the desired signal and there are N_i interfering users. Each signal $s_{kl}(n)$ is given by

$$s_{kl}(n) = \beta_{kl} a_k(n), \tag{35}$$

where $a_k(n)$ is the information symbol that is transmitted by the kth user at time n and β_{kl} is the complex channel gain associated with the kth user's signal and the lth branch. We assume that the amplitude of each channel gain has Rayleigh distribution with $E\{|\beta_{kl}|^2\} = 2\sigma_k^2$ and different users' channel gains are independent of each other.

Representing the signals at the D antenna branches in vector form, we have

$$\underline{r}(n) = \underline{\beta}_0 a_0(n) + B\underline{a}_I(n) + \underline{v}(n), \tag{36}$$

where

$$\begin{aligned}
\underline{r}(n) &= (r_1(n)\, r_2(n)\, \ldots r_D(n))^T, \\
\underline{\beta}_k &= (\beta_{k1}\, \beta_{k2}\, \ldots \beta_{kD})^T, \\
B &= [\underline{\beta}_1\, \underline{\beta}_2\, \ldots\, \underline{\beta}_{N_i}], \\
\underline{a}_I(n) &= (a_1(n)\, a_2(n)\, \ldots\, a_{N_i}(n))^T, \\
\underline{v}(n) &= (v_1(n)\, v_2(n)\, \ldots\, v_D(n))^T.
\end{aligned}$$

Let's assume that the cochannel interference term at each branch is additional AWGN with variance $\sigma_a^2 \sum_{k=1}^{N_i} 2\sigma_k^2$ where $\sigma_a^2 = E\{|a_k(n)|^2\}$ for all k. Denoting interference plus AWGN term at the lth branch as $z_l(n)$ and assuming interference and AWGN are independent of each other, the variance of $z_l(n)$ is

$$E\{|z_l(n)|^2\} = \sigma_a^2 \sum_{k=1}^{N_i} 2\sigma_k^2 + \sigma_v^2, \tag{37}$$

where $\sigma_v^2 = E\{|v_l(n)|^2\}$. In vector form, the interference plus noise term is given by

$$\underline{z}(n) = (z_1(n)\, z_2(n)\, \ldots\, z_D(n))^T = B\underline{a}_I(n) + \underline{v}(n) \tag{38}$$

and the received signal vector is simplified to

$$\underline{r}(n) = \underline{\beta}_0 a_0(n) + \underline{z}(n). \tag{39}$$

Let's define three kinds of power ratio: signal-to-interference power ratio (C/I) $= \sigma_0^2 / \sum_{k=1}^{N_i} \sigma_k^2$, signal-to- noise power ratio (C/N) $= \sigma_a^2 \sigma_0^2 / \sigma_v^2$, and signal-to-interference plus noise power ratio (C/(I+N))

$$\frac{C}{I+N} = \frac{\sigma_0^2}{\sigma_I^2 + (\sigma_v^2/\sigma_a^2)} = \frac{1}{(C/I)^{-1} + (C/N)^{-1}}, \tag{40}$$

where $\sigma_I^2 = \sum_{k=1}^{N_i} \sigma_k^2$. The received signals at the D antenna branches are combined with appropriate combining factors to maximize the output signal-to-noise plus interference power ratio in the maximal ratio combining. Let g_k be the complex combining factor for the kth branch and $\underline{g} = (g_1\, g_2\, \ldots\, g_D)^H$. Then, the combined output signal $y(n)$ is given by

$$y(n) = \underline{g}^H \underline{r}(n) = \underline{g}^H \beta_0 a_0(n) + \underline{g}^H \underline{z}(n) \tag{41}$$

and the output signal-to-noise plus interference power ratio (SNR) is

$$\text{SNR} = \frac{\sigma_a^2 [\sum_{k=1}^{D} g_k \beta_{0k}]^2}{\sum_{k=1}^{D} E\{|g_k z_k(n)|^2\}} = \frac{\sigma_a^2 [\sum_{k=1}^{D} g_k \beta_{0k}]^2}{\sum_{k=1}^{D} |g_k|^2 \sigma_z^2}. \tag{42}$$

Using the Schwartz inequality,

$$\left[\sum_{k=1}^{D} g_k \beta_{0k}\right]^2 \le \sum_{k=1}^{D} |\sigma_z g_k|^2 \sum_{k=1}^{D} \left|\frac{\beta_{0k}}{\sigma_z}\right|^2, \tag{43}$$

where equality is satisfied only when

$$K\sigma_z g_k = \frac{\beta_{0k}^*}{\sigma_z}, \tag{44}$$

for an arbitrary constant K. So, the maximum SNR is achieved when

$$g_k = \frac{\beta_{0k}^*}{\sigma_z^2} \tag{45}$$

giving the maximum SNR denoted by γ as

$$\gamma = \sigma_a^2 \sum_{k=1}^{D} \frac{|\beta_{0k}|^2}{\sigma_z^2}. \tag{46}$$

Because γ is a function of the channel gain vector β_0 whose elements are independent circular complex Gaussian random variables, the SNR after the maximal ratio combining is a χ^2 random variable with $2D$ degrees of freedom, and its probability density function $f(\gamma)$ is given by

$$f(\gamma) = \frac{1}{(D-1)!\gamma} \left(\frac{\gamma}{\Gamma}\right)^D \exp\left(-\frac{\gamma}{\Gamma}\right), \tag{47}$$

where $\Gamma = \sigma_a^2 (2\sigma_0^2)/\sigma_z^2$ is mean signal-to-noise plus interference power ratio at each branch.

Removing the bias in the maximal ratio combining output in (41) before detection or decoding process,

$$\hat{y}(n) = \frac{y(n)}{\underline{g}^H \underline{\beta}_0} = a_0(n) + \frac{\underline{g}^H \underline{z}(n)}{\underline{g}^H \underline{\beta}_0}. \tag{48}$$

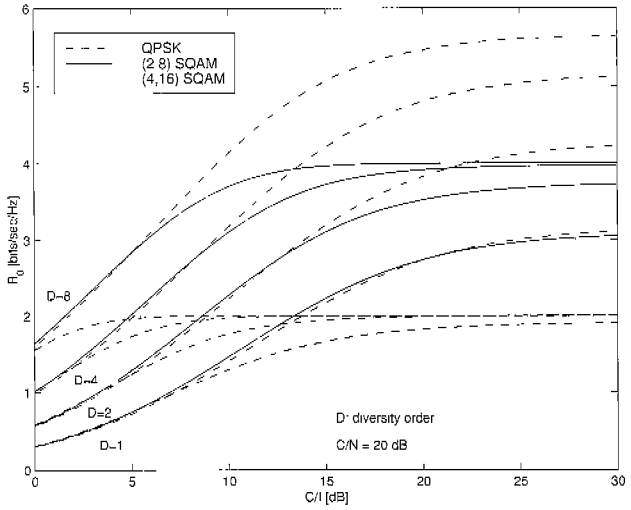

Fig. 13. Average cut-off rate of ACM for different diversity orders when C/N = 20 dB.

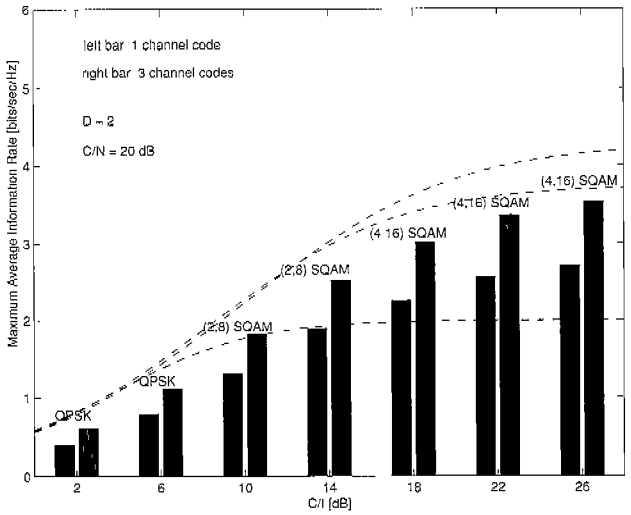

Fig. 14. Maximum average information rate of ACM for diversity order $D = 2$ when C/N = 20 dB.

The second term is AWGN based on the assumptions we made given the channel gain vector for the desired (0th) user's signal, and denoting it as $e(n)$ the variance σ_e^2 is given by

$$E\left\{|e(n)|^2\right\} = \left(\sum_{k=1}^{D} \frac{|\beta_{0k}|^2}{\sigma_z^2}\right)^{-1}. \tag{49}$$

Then, it is easy to show that the pairwise probability of error $P_2(E)$ between two signal points i and j when the signal point i is transmitted is upper-bounded by

$$P_2(E) \leq \exp\left[-\frac{\gamma}{\Gamma}\frac{\sigma_0^2 d_{ij}^2}{4\sigma_z^2}\right], \tag{50}$$

where d_{ij} is the Euclidean distance between the two signal points.

Let's define that $\hat{\gamma} = \gamma/\Gamma$. From (47), the probability density function of $\hat{\gamma}$ can be easily obtained to be

$$\begin{aligned} f(\hat{\gamma}) &= f(\gamma = \Gamma\hat{\gamma}) \\ &= \frac{1}{(D-1)!\,\hat{\gamma}}\,\hat{\gamma}^D \exp(-\hat{\gamma}). \end{aligned} \tag{51}$$

By the way, using the previously defined signal-to-interference power ratio C/I and signal-to-noise power ratio C/N,

$$\frac{\sigma_0^2}{\sigma_z^2} = \frac{1/2}{(\frac{1}{\sigma_a^2}\frac{C}{I})^{-1} + (\frac{C}{N})^{-1}} \tag{52}$$

and the pairwise probability of error in (50) can be rewritten as

$$P_2(E) \leq \exp\left[-\frac{\hat{\gamma}}{8}\frac{d_{ij}^2}{\sigma_a^2(\mathrm{C/I})^{-1} + (\mathrm{C/N})^{-1}}\right]. \tag{53}$$

Following the same argument in Section II, the cut-off rate of ideal adaptive coded-modulation $R_0(\hat{\gamma})$ conditioned on the

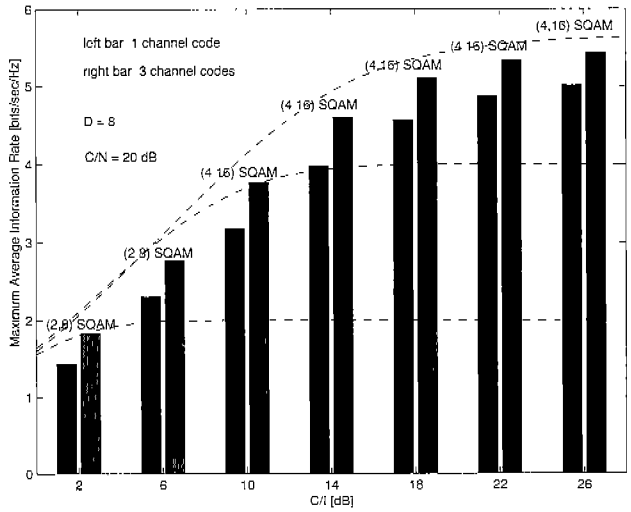

Fig. 15. Maximum average information rate of ACM for diversity order $D = 8$ when C/N = 20 dB.

normalized SNR $\hat{\gamma}$ can be given by

$$R_0(\hat{\gamma}) = -\log_2\left(\frac{1}{M^2}\sum_{i=1}^{M}\sum_{j=1}^{M}\exp\left[-\frac{\hat{\gamma}}{8}\frac{d_{ij}^2}{\sigma_a^2(\mathrm{C/I})^{-1} + (\mathrm{C/N})^{-1}}\right]\right), \tag{54}$$

where M is the cardinality of the modulation signal set, and the average cut-off rate is given by

$$R_0 = \int_0^\infty R_0(\hat{\gamma}) f(\hat{\gamma}) d\hat{\gamma}. \tag{55}$$

Fig. 13 shows the cut-off rate of ACM with the maximal ratio combining for different diversity orders: $D = 1$, 2, 4 and 8. The signal-to-noise power ratio C/N is assumed to be 20 dB, and the cut-off rate is plotted as a function of the signal-to-interference ratio C/I. When C/I ratio is below 20 dB, we have

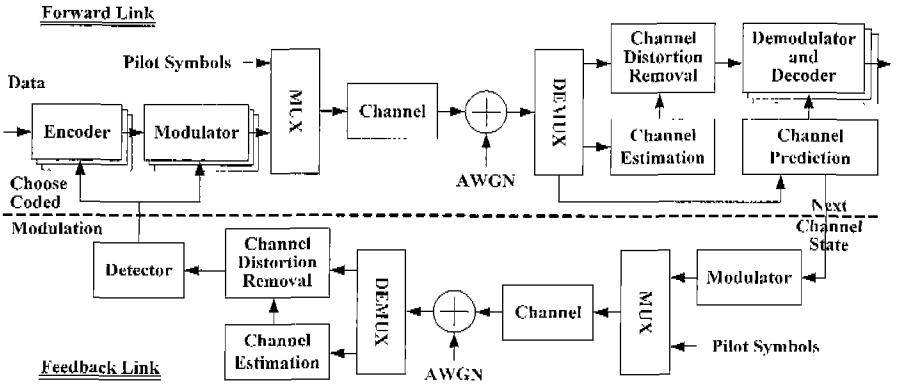

Fig. 16. System block diagram for simulation.

interference-limited situation. As is apparent from the figure, the signal-to-interference region where modulation with high spectral efficiency can provide substantial improvement in the average cut-off rate moves down to lower region as we increase diversity order. Due to the fact that C/N = 20 dB, there is almost no difference in the average cut-off rate between $(2, 8)$ and $(4, 8)$ SQAMs for $D = 1$ even as C/I ratio increases up to 30 dB. This phenomenon also occurs for $D = 2$, 4 and 8 until C/I ratio is below 15, 10 and 5 dB, respectively. This implies that optimal modulation should be selected carefully depending on the diversity order, C/N ratio and C/I ratio. In Fig. 14 and 15, we show the maximum average information rate of practical ACM schemes with 1 and 3 channel code(s) for diversity order $D = 2$ and $D = 8$, respectively. The left bar denotes the maximum average information rate of ACM with single channel code, and the right one with 3 channel codes. The signal-to-noise power ratio (C/N) is assumed to be 20 dB for both cases. On the top of each bar, modulation used for the transmitted waveform is indicated, which is decided based on the result in Fig. 13. Also the cut-off rate curves of ideal ACM in Fig. 13 are shown in dotted lines. Since the probability of deep fades diminishes as we increase the diversity order, it is of interest to see how much improvement we can achieve by employing multiple channel codes instead of single one in adaptive coded-modulation. In other words, the trade-off between performance gain and system complexity is of interest. As observed in comparing the two figures, the improvement obtained with 3 channel codes becomes smaller when the diversity order is increased to $D = 8$ from $D = 2$. It is conjectured that as the diversity order is increased to infinity the cut-off rate curve of ACM will be flat over the signal-to-interference power ratio (C/I) of interest given C/N ratio and the flat level of the average cut-off rate will be determined by the C/N ratio. This implies that given the C/N ratio single channel code will be enough for ACM with high diversity order. On the other hand, the gap between the average cut-off rate of ideal ACM and the maximum average information rate of practical ACM is decreasing as the diversity order increases.

VI. SIMULATION STUDY OF ACM

Up to now, advantages gained by using adaptive coded-modulation have been discussed with idealistic assumptions for analytic simplicity. To demonstrate the adaptive coded-modulation in more realistic environments, computer simulation is used so as to assess various constraints and limitations expected to be encountered in practical implementation of adaptive coded-modulation. Such constraints and limitations include: errors in feedback of channel state information, errors in channel state estimation and prediction, effects of automatic request retransmission (ARQ) which is necessary to improve the radio link reliability, and so on.

A. Simulation Model

A.1 System Model

In Fig. 16, system block diagram used for simulation is illustrated. Multiple coded-modulations are available at the transmitter, and for a given transmission block a coded-modulation is chosen depending on the fed-back channel state information.

The channel is assumed to be flat Rayleigh fading, and is generated based on the Jakes' model [15]. Simulation is based on a baseband model with pulse shaping and matched filtering absorbed into the channel, and the received signal r_k at time k is given by $r_k = \beta_k s_k + n_k$ where β_k is the complex multiplicative distortion introduced by the channel, s_k is the transmitted channel symbol, and n_k is additive white Gaussian noise (AWGN). For different modulations, it is assumed that the transmitted signal s_k has the same peak energy E_s. The variance of β_k is normalized to be 1, and when the AWGN has two-sided power spectral density $N_0/2$ the variance of n_k is given by $E(|n_k|^2) = 1/(E_s/N_0)$.

A block of received signal is processed to estimate the channel distortion β_k and to predict the channel state for next transmission block. The estimation and prediction methods are described in detail in next section while discussing frame structure. Demodulation and decoding are followed after the channel distortion is eliminated.

A.2 Frame Structure

The frame structure assumed for simulation is illustrated in Fig. 17. Each frame consists of N_{sl} slots, and the frame duration is T_F. A pilot symbol is assigned to the first symbol of each slot, which is used for channel estimation and prediction. A coded-modulation is associated with each frame, and in the

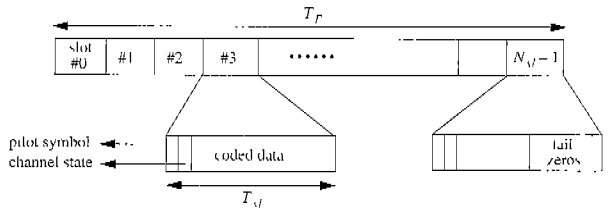

Fig. 17. Frame structure.

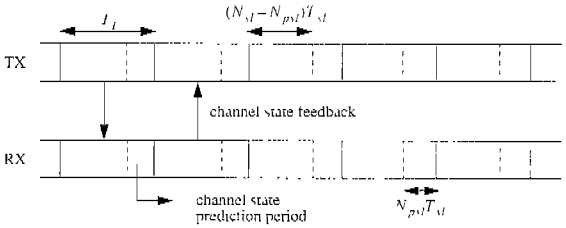

Fig. 18. Channel state feedback method.

feedback link the channel state information is also multiplexed after the pilot symbol. The duration of each slot is T_{sl}. When convolutional code or trellis coded-modulation (TCM) is used for channel encoding, tailing zeros are appended in the last slot.

Estimation of the channel-induced distortion β_k is based on linear interpolation using the pilot symbols. When there are N_s symbols per each slot, the estimate of β_k, where $lN_s \leq k < (l+1)N_s$, can be obtained by

$$\hat{\beta}_k = \hat{\beta}_{lN_s} + \Delta_l(k - lN_s), \tag{56}$$

where $\hat{\beta}_{lN_s}$ at pilot symbol position is given by

$$\hat{\beta}_{lN_s} = r_{lN_s}/s_k \tag{57}$$

and the slope

$$\Delta_l = \left(\hat{\beta}_{(l+1)N_s} - \hat{\beta}_{lN_s}\right)/N_s. \tag{58}$$

The received signal r_k is divided by $\hat{\beta}_k$, and $z_k = r_k/\hat{\beta}_k$ used for demodulation and decoding.

Channel state feedback operation is illustrated in Fig. 18. First N_{psl} slots in each frame are used for channel state prediction, and that information is transmitted back using the following frame. The reason for using just N_{psl} slots for the prediction is that we need processing time for channel state prediction. In this manner we can reduce feedback delay. If we try to use N_{sl} slots for prediction, the following frame right after the prediction can not be used for feedback resulting in longer feedback delay, while using more pilot symbols can improve the accuracy of channel state prediction.

The algorithm used in channel state prediction is based on the least mean square method [13]. New observation u, which is input to the prediction filter, is given by

$$u = \frac{1}{N_{psl}} \sum_{l=0}^{N_{psl}-1} \hat{\beta}_{lN_s}, \tag{59}$$

as discussed in Section IV. A training period is assumed at the initial launch of every simulation to make the prediction filter coefficients converge.

B. Simulation Results

Three coded-modulations are considered to compare the throughput performance of ACM and fixed coded-modulation (FCM): convolutional code of code rate 1/2 with QPSK (CODE1), trellis coded-modulation (TCM) with 16 QAM (CODE2), and TCM with 64 QAM (CODE3). All three channel codes have the same constraint length of 5. ACM selects one of three codes depending on the channel state. Channel symbol rate is assumed to be 64 ksps for all the results. Stop-and-Wait ARQ is used for retransmission scheme.

Fig. 19 shows the throughput of ACM and 3 FCMs when the maximum Doppler frequency D_f is 10 Hz. Over the entire range of SNR levels considered, ACM outperforms all the FCMs in throughput.

Fig. 20 shows the throughput of ACM and CODE1 for different D_f values. Even when the maximum Doppler frequency is increased to 50 Hz, ACM still outperforms CODE1. As the maximum Doppler frequency increases, degradation in the throughput performance of ACM is much larger than FCM, and it is conjectured that increase in channel state prediction error is the main cause of the degradation.

Fig. 21 shows the throughput performance of ACM and CODE1 with different diversity orders. Maximal ratio combining is used at the receiver based on the multiplicative distortion estimation at each diversity branch. It is assumed that each diversity path has equal average signal strength. With CODE1, the throughput is almost doubled when the order of the diversity is increased from 1 to 2 while there is a minimal increase in throughput when the order of diversity is increased from 2 to 4. However, with ACM, we always observe a substantial improvement in throughput as the order of the diversity increases. It is because ACM can use more spectrally-efficient coded-modulation as the channel condition improves.

VII. CONCLUSION

In this paper, we demonstrated that the adaptive coded-modulation can improve the spectral efficiency substantially in slowly varying fading channels where interleaving is not effective. Cut-off rate analysis was used extensively to evaluate the spectral efficiency of ACM under ideal conditions and to show that channel prediction can be an effective way in overcoming channel dynamics. Also, throughput performance of ACM was studied by computer simulation to assess the effects of channel estimation/prediction errors and channel state feedback errors. The simulation results demonstrate that even with this errors unavoidable in practice, ACM provide a significant improvement in throughput compared to the conventional fixed coded-modulation.

The adaptive coded-modulation is a promising and efficient way to meet the throughput demand for next generation wireless communications systems.

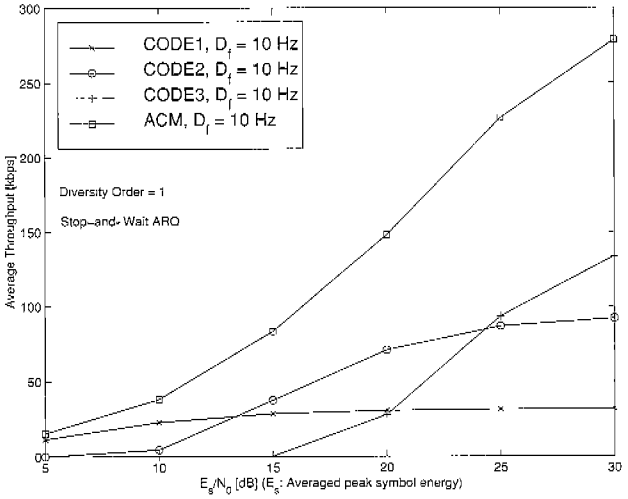

Fig. 19. Throughput of ACM and FCMs when $D_f = 10$ Hz with Stop-and-Wait ARQ.

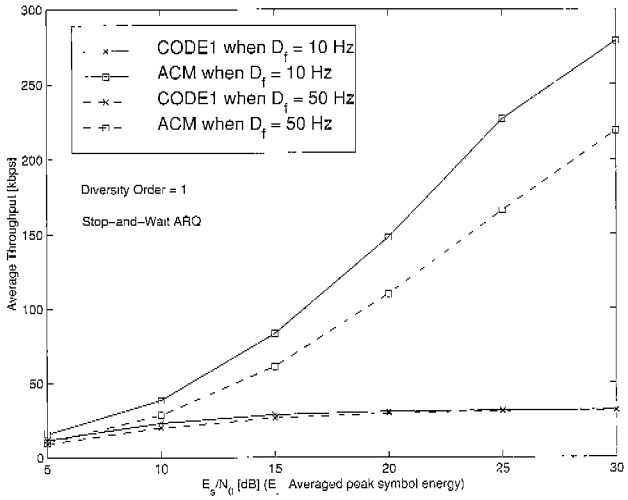

Fig. 20. Throughput of ACM and CODE1 for different D_f values with Stop-and-Wait ARQ.

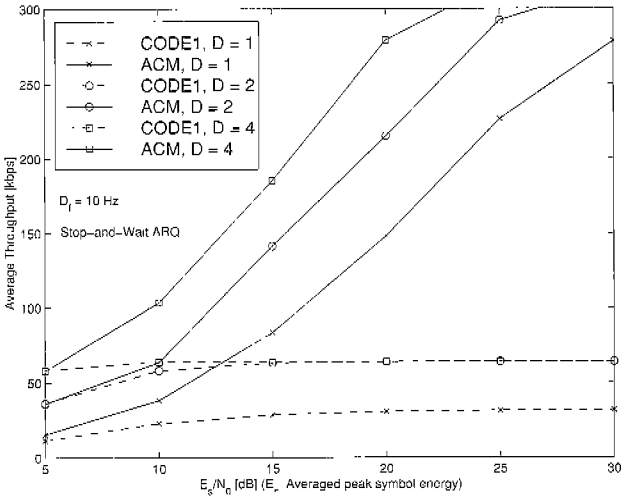

Fig. 21. Throughput of ACM and CODE1 for different orders of diversity with $D_f = 10$ Hz and Stop-and-Wait ARQ.

REFERENCES

[1] J. Hancock and W. Lindsey, "Optimum performance of self-adaptive systems operating through a Rayleigh-fading medium," *IEEE Trans. Commun.*, pp. 443–453, Dec. 1963.

[2] S. Chia, "The universal telecommunication system," *IEEE Commun. Mag.*, pp. 54–62, Dec. 1992.

[3] W. Webb and R. Steele, "Variable rate QAM for mobile radio," *IEEE Trans. Commun.*, pp. 2223–2230, July 1995.

[4] W. Webb, "Spectrum efficiency of multilevel modulation schemes in mobile radio communications," *IEEE Trans. Commun.*, pp. 2344–2349, Aug. 1995.

[5] N. Morinaga, M. Nakagawa, and R. Kohno, "New concepts and technologies for achieving highly reliable and high-capacity multimedia wireless communications systems," *IEEE Commun. Mag.*, pp. 34–40, Jan. 1997.

[6] A. Goldsmith and S. Chua, "Variable-rate variable-power MQAM for fading channels," *IEEE Trans. Commun.*, pp. 1218–1230, Oct. 1997.

[7] W. Webb, L. Hanzo, and R. Steele, "Bandwidth efficient QAM schemes for rayleigh fading channels," *IEE Proc.-I*, pp. 169–175, June 1991.

[8] T. Ikeda, S. Sampei, and N. Morinaga, "TDMA Based adaptive modulation with dynamic channel assignment (AMDCA) for large capacity voice transmission in microcellular systems," *Electron. Lett.*, vol. 32, no. 13, pp. 1175, June 1996.

[9] A. Goldsmith and P. Varaiya, "Capacity of fading channels with channel side information," *IEEE Trans. Info. Theory*, pp. 1986–1992, Nov. 1997.

[10] M. Simon, S. Hinedi, and W. Lindsey, *Digital Communication Techniques*, Prentice Hall, 1995.

[11] J. Massey, "Coding and modulation in digital communications," in *Proc. Zurich Seminar*, pp. E2(1)–E2(4), 1974.

[12] J. Wozencraft and R. Kennedy, "Modulation and demodulation for probabilistic coding," *IEEE Trans. Inform Theory*, pp. 291–297, July 1966.

[13] S. Haykin, *Adaptive Filter Theory*, 3rd ed., Prentice Hall, 1996.

[14] M. Schwartz, W. R. Bennett and S. Stein, *Communication Systems and Techniques*, McGRAW-Hill, 1966.

[15] W. C. Jakes (Ed.), *Microwave Mobile Communications*, New York: Wiley, 1974.

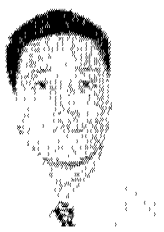

Young Min Kim was born in Seoul, Korea, in 1966. He received the B.S. degree from Seoul National University, Korea, in 1990, the M.S. degree from Virginia Tech., VA, U.S.A., in 1995, all in electrical engineering. He is pursuing the Ph.D. degree in electrical engineering at University of Southern California, Los Angeles, CA, U.S.A. Currently he is with LinCom Corporation, Los Angeles, CA, U.S.A. His area of interest is wireless communications system design. He is a member of IEEE.

William C. Lindsey is a Professor of Electrical Engineering at the University of Southern California, and serves as Chairman of the Board of LinCom Corporation which he founded in 1974. He has been a frequent consultant to government and industry. He has published numerous papers on varied topics in communication theory and holds several patents. He has written three books: Synchronization Systems in Communication and Control (Englewood Cliffs, NJ: Prentice-Hall, 1972); Telecommunication Systems Engineering, co-authored with M.K. Simon (Englewood Cliffs, NJ: Prentice Hall, 1973; revised edition, Dover Publications, 1991); Digital Communication Techniques: Signal Design and Detection, co-authored with Marvin K. Simon and Sami M. Hinedi (Englewood Cliffs, NJ: Prentice Hall ,1995). He is also coauthor of the IEEE Press Book Phase-Locked Loops and Their Applications.

Dr. Lindsey serves on Commission C, Signals and Systems of the International Scientific Radio Union (URSI) and was Vice President for Technical Affairs of the IEEE Communications Society. He also served as the second chairman of the Communication Society and is a former Editor of ComSoc. Currently he serves as an editor for the Journal on Communications and Networks.

Dr. Lindsey is a Fellow of the IEEE. He is a member of the National Academy of Engineering (NAE).